B Cell Response After MMTV Infection: Extrafollicular Plasmablasts Represent the Main Infected Population and Can Transmit Viral Infection[1]

Carlos Ardavín,[2]*‡ Pilar Martín,‡ Isabel Ferrero,‡ Iñigo Azcoitia,‡ Fabienne Anjuère,‡ Heidi Diggelmann,§ Frédéric Luthi,§ Sanjiv Luther,*† and Hans Acha-Orbea[3]*†

The immune response to mouse mammary tumor virus (MMTV) relies on the presentation of an MMTV-encoded superantigen by infected B cells to superantigen-specific T cells. The initial extrafollicular B cell differentiation involved the generation of B cells expressing low levels of B220. These B220^{low} B cells corresponded to plasmablasts that expressed high levels of CD43 and syndecan-1 and were CD62 ligand$^-$ and IgD$^-$. Viral DNA was detected nearly exclusively in these B220^{low} B cells by PCR, and retroviral type-A particles were observed in their cytoplasm by electron microscopy. An MMTV transmission to the offspring was also achieved after transfer of B220^{low} CD62 ligand$^-$ CD43$^+$ plasmablasts into noninfected females. These data suggest that B220^{low} plasmablasts, representing the bulk of infected B cells, are capable of sustaining viral replication and may be involved in the transmission of MMTV. *The Journal of Immunology,* **1999, 162: 2538–2545.**

Mouse mammary tumor virus (MMTV)[4] is a B-type retrovirus that, upon infection of the mammary gland epithelial cells, promotes the development of mammary carcinomas by insertional activation of host protooncogenes (reviewed in Ref. 1).

MMTV is transmitted through milk to newborn mice during the first 2 wk of life by initially infecting B cells in the Peyer's patches (2). Efficient MMTV infection is dependent upon the presentation of an MMTV-encoded superantigen (SAg) by the initial pool of infected B cells to SAg-reactive T cells (3). The resulting SAg-specific Th cell response, mediated by the cross-linking of B cell MHC class II molecules with TCR Vβ elements, leads to the amplification of the infected cells by inducing a strong B cell proliferation and differentiation response (4). Immunohistochemical analysis of the draining lymph node after infection with MMTV has demonstrated that MMTV-SAg drives extrafollicular and follicular B cell differentiation, following a very similar pattern to that described for conventional Ags (5).

The follicular phase of a B cell response comprises a complex series of events occurring during the germinal center reaction, implying the somatic hypermutation of Ig genes and the selection of high-affinity mutants (6). In contrast, extrafollicular B cell differentiation involves an early Ag-specific proliferation and differentiation of B cells taking place within the so-called extrafollicular foci and leading to the generation of a first wave of plasmablasts (7). These extrafollicular plasmablasts appear to display low levels of B220 and to express the proteoglycan molecule syndecan-1 (CD138) (8, 9). Interestingly, although plasma cells have been considered to be short-lived cells, two recent reports have demonstrated that a substantial fraction of them can survive for periods of >1 yr (10, 11).

Previous reports have demonstrated that very few B cells are infected in the first days after MMTV injection. It was estimated that in the draining popliteal lymph node (PO-LN), ~1 of 10,000 B cells were infected 48 h after injection of the Swiss strain of MMTV, MMTV(SW), into the footpad of BALB/c mice (12). However, between days 2 and 6 (i.e., during the extrafollicular phase of the B cell response), the number of infected B cells increases >1000-fold by cell division-mediated expansion of the initial number of infected cells. This SAg-mediated B cell response has been demonstrated to be required for a successful MMTV infection of the mammary gland (3, 13). However, the mechanism of virus transmission to the mammary gland is still largely unknown, because the data dealing with the capacity of different lymphocyte subsets to transmit MMTV infection after transfer into appropriate hosts remain controversial (reviewed in Ref. 14). In addition, it has been reported that under physiological conditions, large quantities of new virus particles are not produced during the first phase of infection, but only by the infected epithelial cells of the mammary and salivary glands under the control of the endocrine system by pregnancy hormones (reviewed in Ref. 15). Finally, the characterization of the cell type responsible for virus transfer to the mammary gland is further complicated by virus spread from the initially infected B cells to T cells (16). Therefore, to get new insights on the transmission of the virus to the mammary gland, we have extensively analyzed the B cell response induced upon infection by MMTV(SW). Our results support the hypothesis that the MMTV(SW)-infected plasmablasts differentiated during the early extrafollicular B cell response, which can be

*Ludwig Institute for Cancer Research, Lausanne Branch, and †Institute for Biochemistry, University of Lausanne, Epalinges, Switzerland; ‡Department of Cell Biology, Faculty of Biology, Complutense University, Madrid, Spain; and §Institute of Microbiology, University of Lausanne, Lausanne, Switzerland

Received for publication April 1, 1998. Accepted for publication October 30, 1998.

The costs of publication of this article were defrayed in part by the payment of page charges. This article must therefore be hereby marked *advertisement* in accordance with 18 U.S.C. Section 1734 solely to indicate this fact.

[1] This work was supported by Grant RP12-95 from the Fundación Eugenio Rodríguez Pascual to C.A., by Grant 31-32271.94 from the Swiss National Science Foundation, and by Grant RG-544/95 from the Human Frontiers of Science Program to H.A.-O.

[2] Current address: Dr. Carlos Ardavín, Department of Cell Biology, Faculty of Biology, Complutense University, 28040 Madrid, Spain.

[3] Address correspondence and reprint requests to Dr. Hans Acha-Orbea, Ludwig Institute for Cancer Research, Lausanne Branch and Institute for Biochemistry, University of Lausanne, 1066 Epalinges Switzerland. E-mail address: hacha@eliot.unil.ch

[4] Abbreviations used in this paper: MMTV, mouse mammary tumor virus; PO-LN, popliteal lymph node(s); MS-LN, mesenteric lymph node(s); CD62L, CD62 ligand; SAg, superantigen; LTR, long terminal repeat; ORF, open reading frame; PE, phycoerythrin; SA, streptavidin; FSC, forward scatter.

0022-1767/99/$02.00

identified and therefore traced during the infection process on the basis of its phenotypic profile and which may be involved in MMTV transmission to the mammary gland and to the offspring.

Materials and Methods

Mice

BALB/c mice were purchased from Harlan Olac (Bicester, U.K.). In all experiments, 8- to 10-wk-old mice were used.

Antibodies

The following Abs were used in this study: FD11-54-3 (anti-MHC class II, biotin-conjugated; Ref. 17), H1-2F3 (anti-CD69, biotin-conjugated; Ref. 18), FD44.8 (anti-LFA-1α, biotin-conjugated; Ref. 17), Mel-14 (anti-CD62 ligand (CD62L), biotin-conjugated; Ref. 19), IM7.81 (anti-CD44, biotin-conjugated; Ref. 20), FGK45 (anti-CD40, biotin-conjugated; Ref. 21), 44-22.1 (anti-Vβ6, fluorescein-conjugated; Ref. 22), GL1 (anti-B7-2, biotin-conjugated; PharMingen, San Diego, CA), S7 (anti-CD43, biotin-conjugated; PharMingen), 281-2 (anti-syndecan-1, biotin-conjugated; PharMingen), AMS9.1 (anti-IgD, biotin-conjugated; PharMingen), LO-MM (anti-IgM, biotin-conjugated; Caltag, San Francisco, CA), RA3-6B2 (anti-B220, FITC-conjugated; Caltag), H129.19 (anti-CD4, phycoerythrin (PE)-conjugated; Boehringer Mannheim, Mannheim, Germany), 53-6.7 (anti-CD8, PE-conjugated; Boehringer Mannheim), and M5-114 (anti-MHC class II, PE-conjugated; Boehringer Mannheim).

Virus isolation and in vivo treatment

MMTV(SW) was purified from milk as described previously (4). Mice were given a 10 μl injection in the hind footpad with MMTV(SW) (10^9 virus particles, titered as described in Ref. 3). After the indicated times, the popliteal, inguinal, and mesenteric lymph nodes, spleen, and Peyer's patches were removed, and single cell suspensions were prepared.

Flow cytometry

The kinetics of B cell and T cell activation as well as the percentage of Vβ6$^+$ T cells were analyzed after triple-staining with biotinylated anti-CD69, followed by streptavidin (SA)-tricolor (Caltag, San Francisco, CA), PE-conjugated anti-CD4 and anti-CD8, and fluoresceinated anti-Vβ6. CD4$^+$ and CD8$^+$ cells were separated in the FL2 channel using appropriate dilutions of the two mAbs. Analysis of the B220^{low} and B220^{high} B cells was performed after triple-staining with biotinylated mAbs against CD69, IgM, IgG2a, IgD, CD62L, CD43, syndecan-1, LFA-1, and CD44, followed by SA-tricolor (Caltag), PE-conjugated anti-MHC class II, and fluoresceinated anti-B220. Analysis was performed on a FACScan (Becton Dickinson, Mountain View, CA) cell analyzer, using Lysys II software for data evaluation.

MHC class II$^+$ B220^{low} and MHC class II$^+$ B220^{high} B cells from the draining PO-LN were FACS-sorted 6 days after MMTV injection on a FACStar (Becton Dickinson) flow cytometer after double staining with biotinylated anti-MHC class II followed by SA-PE (Caltag) and fluoresceinated anti-B220. After reanalysis, the sorted cell populations had a purity of >99% (data not shown).

Cell cycle analysis

The cell cycle was analyzed on FACS-sorted MHC class II$^+$ B220^{low} or MHC class II$^+$ B220^{high} B cells by cell nuclei DNA staining with propidium iodide (50 μg/ml), 0.1% Triton X-100, and 0.1% sodium citrate as described by Nicoletti et al. (23). The percentage of apoptotic and blast cells within B cells was estimated on the basis of the forward scatter (FSC).

Polymerase chain reaction

DNA of 50,000 FACS-sorted MHC class II$^+$ B220^{low} or MHC class II$^+$ B220^{high} B cells (purity of >99%) was amplified with MMTV long terminal repeat (LTR) oligonucleotides that do not allow the distinction between endogenous and exogenous MMTV sequences. The individual MMTV sequences can be distinguished based on the length differences of the amplified fragments, with Mtv-6 giving the shortest, Mtv-8 and -9 the intermediate, and MMTV(SW) the longest fragments in MMTV(SW)-infected BALB/c mice. The oligonucleotides to amplify all LTR-sequences were chosen on the basis of the high degree of conservation between the 3′ LTR-open reading frames (ORFs). To amplify Mtv ORFs from all Mtv-DNAs, the 5′ oligonucleotide ORF-100 (CTCAGGAAGAAAAA GACGACAT) was used in combination with the 3′ oligonucleotide VJ71 (CCCAAACCAAGTCAGGAAACCACTTG), yielding a 250–290-kb PCR product. For PCR, the conditions were: 5 min at 95°C, followed by 40 cycles of 1 min at 60°C, 1 min at 72°C, and 30 s at 95°C, and finally 7 min at 72°C in 1 × PCR buffer containing 20 mM Tris-HCl (pH 8.55), 16 mM $(NH_4)_2SO_4$, 2.5 mM $MgCl_2$, 150 μg/ml BSA, and 0.2 mM of each of the four 2′-deoxynucleoside 5′-triphosphates (dNTPs). A total of 2.5 U of *Taq* polymerase (BioTaq; Bioprobe Systems, Montreuil, France), 3 μCi of [α-^{32}P]dATP (New England Biolabs, Beverly, MA), and 0.5 μM of each oligonucleotide were added per PCR. PCR products were separated on 6% polyacrylamide gels, and the dried gels were autoradiographed on Kodak X-OMAT films (Eastman Kodak Company, Rochester, NY).

Light and electron microscopy

After the indicated survival times, the PO-LN or B220^{low} B cells sorted from PO-LN 6 days after MMTV(SW) injection were fixed with 1% glutaraldehyde and 1% paraformaldehyde in 0.1 M (pH 7.6) Sørensen phosphate buffer for 16 h at 4°C, postfixed with 1% OsO4 in the same buffer for 1 h at 4°C, dehydrated in graded acetone solutions, and embedded in Araldite. Semithin sections (1 μm) were stained with toluidine blue and photographed in an Zeiss Axioskop microscope (Zeiss, Oberkochen, Germany); ultrathin sections (70–80 nm) were counterstained with uranyl acetate and lead citrate and examined with a Jeol 1010 electron microscope (Tokyo, Japan).

Transfer of MMTV infection

B220^{low} CD62L$^-$ CD43$^+$ plasmablasts, B220^{high} CD62L$^+$ CD43$^-$ B cells, or total T cells were isolated from the draining PO-LN of BALB/c mice 6 days after MMTV injection. For this assay, the purification of the B220^{low} and B220^{high} B cell subsets was performed on the basis of the expression of CD62L and CD43, as a small proportion of CD62L$^-$ CD43$^+$-responding blast cells that have not yet undergone the down-regulation of B220 and could be infected by MMTV exists within the B220^{high} B cell population at 6 days after infection with MMTV (see Fig. 2*B*). CD62L− CD43+ plasmablasts and CD62L+ CD43− B cells were purified by magnetic cell sorting with MACS separation columns (Miltenyi Biotec, Bergisch, Germany) after T cell depletion by complement mediated cytotoxicity. For this purpose, purified total B cells obtained after T cell depletion (purity >97%) were incubated with biotinylated anti-CD43 or anti-CD62L mAbs, followed by streptavidin-conjugated MACS microbeads (Miltenyi Biotec). After reanalysis, the purified CD62L$^-$ CD43$^+$ and CD62L$^+$ CD43$^-$ B cell populations had a purity of >98% (data not shown). Therefore, the small proportion of CD62L$^-$ CD43$^+$ B220^{high} blast B cells (see Fig. 2*B*), which could potentially contain MMTV-infected cells, is included in the CD62L$^-$ CD43$^+$ subset, but absent from the CD62L$^+$ CD43$^-$ B cell subpopulation. A total of 5×10^5 purified CD62L$^-$ CD43$^+$ plasmablasts, CD62L$^+$ CD43$^-$ B cells, or total T cells from day 6 MMTV(SW)-injected mice or total PO-LN cells from noninfected control mice were transferred i.v. into BALB/c females, which were then crossed with noninfected BALB/c males. Deletion of circulating Vβ6$^+$ CD4$^+$ T cells in the mothers and their offspring was monitored at the indicated times. Blood leukocytes were removed by tail bleeding from heparinized blood samples by centrifugation through a Ficoll (Pharmacia, Uppsala, Sweden) cushion, and stained with PE-conjugated anti-CD4 and fluoresceinated anti-Vβ6.

Results

Analysis of responding B cells during MMTV infection

Injection of MMTV(SW) into the footpad of BALB/c mice induced a strong B cell and T cell proliferative response in the draining PO-LN, as assessed by the analysis of the percentage of cycling cells and of B and T blast cells (data not shown). As previously reported, B cells underwent a biphasic activation: an initial transient T cell-independent B cell activation, occurring within the first 24 h, was followed by a second B cell activation phase starting 2 days after infection and reaching a peak by day 4 (24). This second B cell activation phase was accompanied by a strong B cell proliferative response that amplified the initial number of infected B cells and required the presentation by the infected cells of an MMTV(SW)-encoded SAg to the SAg-reactive Th cells (3).

Analysis of the B220 vs MHC class II expression of the B cells during the B cell response revealed the appearance by day 4 of a B cell subpopulation expressing MHC class II levels that were similar to those of control mice, but lower B220 expression (Fig. 1*A*). This B220^{low} B cell population, hardly detectable in the

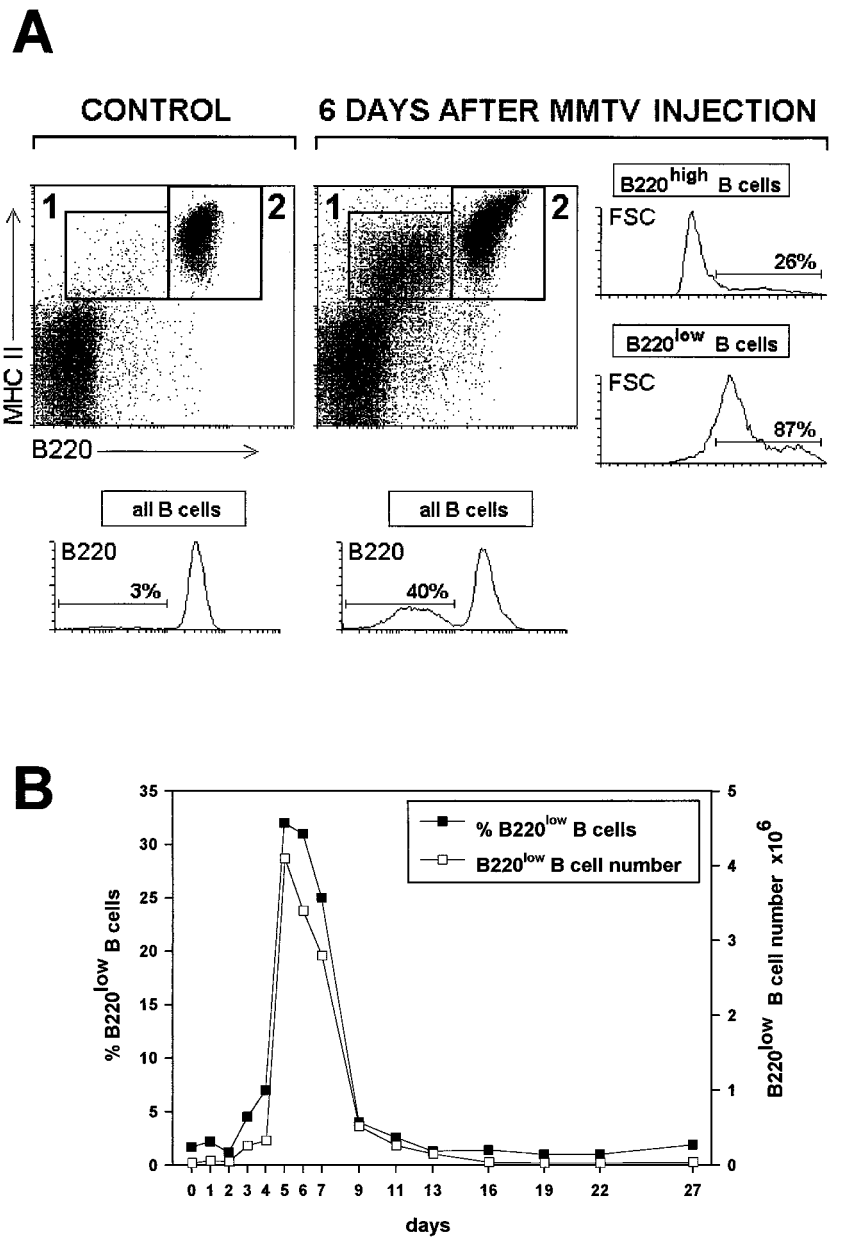

FIGURE 1. Analysis of early B cell differentiation after MMTV(SW) injection. *A*, Dot plots show the B220 vs MHC class II profiles of PO-LN cells from control mice and from mice at day 6 after MMTV(SW) injection. Boxes define $B220^{low}$ (1) and $B220^{high}$ (2) B cells. Histograms represent the B220 expression within the total B cell population in control mice and in MMTV(SW)-injected mice at day 6 and the FSC of $B220^{low}$ and $B220^{high}$ B cells. The percentage of $B220^{low}$ cells within the total B cell population and the percentage of blast cells (FSC >130) are shown for the indicated cell subsets. *B*, Analysis of $B220^{low}$ B cells during the immune response to MMTV(SW). The percentage of $B220^{low}$ cells within total B cells and the absolute number of $B220^{low}$ B cells per draining PO-LN are shown for the indicated time points after MMTV(SW) injection. The data are representative of four experiments with similar results.

PO-LN of control mice, in which it represented $<3\%$ of the total B cells (Fig. 1*A*), reached a maximum by days 5 and 6, when it constituted $\leq 40\%$ of the B cell subset, and returned to control levels by day 11 in the PO-LN of MMTV(SW)-infected mice (Fig. 1*B*). Therefore, the kinetics of the $B220^{low}$ B cells paralleled the B cell activation and proliferation response induced by MMTV(SW). At 6 days after virus injection, the $B220^{low}$ B cell population represented $\leq 40\%$ of the total lymph node B cells (i.e., $4–5 \times 10^6$ cells) and contained $\leq 90\%$ of blast cells, whereas only $\sim 25\%$ blast cells were detected in the $B220^{high}$ B cell population (Fig. 1*A*). Analysis of the cell cycle of the $B220^{low}$ and $B220^{high}$ B cell subpopulations sorted by FACS (Fig. 2) showed that, although the $B220^{high}$ B cell population had a basal level of cycling cells (3%), the $B220^{low}$ B cells displayed a high percentage of proliferating cells (19% cycling cells). These results indicate that the $B220^{low}$ MHC class II^+ B cell subpopulation contains the vast majority of the dividing B cells during the SAg-mediated B cell response induced by MMTV(SW).

Analysis of the phenotype of $B220^{low}$ and $B220^{high}$ B cells

As shown in Fig. 2, the analysis of cell surface marker expression by the $B220^{low}$ and $B220^{high}$ B cells revealed important phenotypic differences between both B cell subpopulations. $B220^{low}$ B cells expressed high levels of the B cell differentiation markers CD43 and syndecan, whereas only a small proportion of $B220^{high}$ B cells expressed these markers. $B220^{low}$ B cells did not express surface IgDs, whereas $B220^{high}$ B cells were IgD^+. Correspondingly, $B220^{low}$ B cells were negative for the homing molecule CD62L (L-selectin), whereas $B220^{high}$ B cells were $CD62L^+$. In addition, $B220^{low}$ B cells underwent a strong CD44 up-regulation and displayed higher LFA-1 levels than the $B220^{high}$ cells. Finally, $\sim 40\%$ of $B220^{high}$ B cells were positive for the early activation marker CD69, but this marker was down-regulated in the $B220^{low}$ B cells. The phenotype of $B220^{low}$ B cells corresponds to that of plasmablasts, originated by extrafollicular differentiation of MMTV-responding B cells, which have switched to downstream

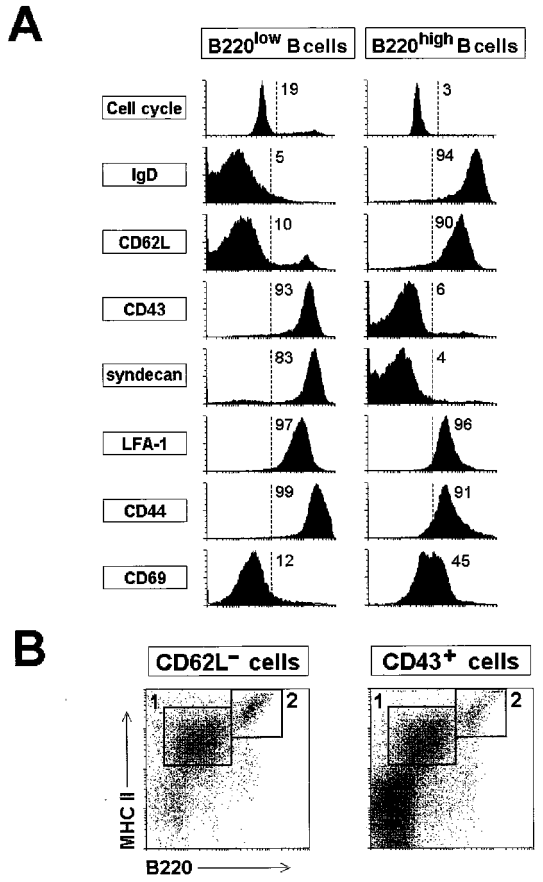

FIGURE 2. Phenotype of B220^{low} plasmablasts and B220^{high} B cells in the draining PO-LN 6 days after MMTV(SW) injection. *A*, Histograms represent the cell cycle and cell surface marker expression of B220^{low} and B220^{high} B cells. Cell cycle analysis was performed on sorted B220^{low} and B220^{high} B cells as described previously. The percentage of cycling cells (FL3 >140 on a linear scale) for each population is indicated. Cell surface marker expression of the indicated markers was analyzed after triple-staining with biotinylated mAbs followed by SA-tricolor, FITC-conjugated anti-B220, and PE-conjugated anti-MHC class II. The percentage of positive cells (FL3 $>10^2$ on a logarithmic scale) for each marker is indicated. These data are representative of three to five experiments with similar results. *B*, Dot plots represent the B220 vs MHC class II profiles of CD62L$^-$ and CD43$^+$ PO-LN cells from mice at day 6 after MMTV(SW) injection. Boxes define B220^{low} (1) and B220^{high} B cells (2). B220^{high} B cells represented ~8–10% of the CD62L$^-$ or CD43$^+$ B cells.

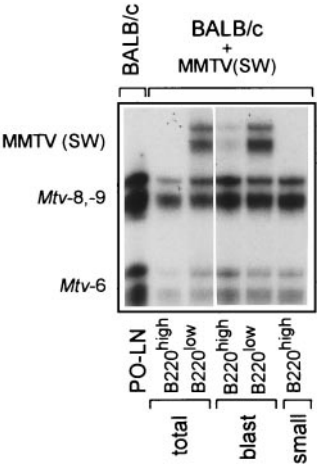

FIGURE 3. Detection of viral DNA by PCR. DNA was amplified from the indicated cell subsets and obtained from control mice or mice at day 6 after MMTV(SW) injection using primers specific for endogenous as well as exogenous MMTV sequences. The individual MMTV sequences were distinguished on the basis of the length differences of the amplified fragments. No viral DNA was detected in total PO-LN cells from control BALB/c mice or total B220^{high} B cells from day 6 PO-LN, whereas a strong signal was obtained for B220^{low} plasmablasts. Viral DNA could be detected in blast but not small B220^{high} B cells, indicating that a small proportion of MMTV-infected blast B cells existed within the B220^{high} B cell subset. Most likely, these cells corresponded to a small proportion of CD62L$^-$ CD43$^+$ blast B cells that had not down-regulated B220 by day 6 after MMTV(SW) injection.

Ig classes. Therefore, B220^{low} B cells will hereafter be referred to as B220^{low} plasmablasts.

The kinetics of the B cell response, induced by MMTV as shown in Fig. 1, and the phenotypic characteristics of responding B cells described above indicate that B220^{high} B cells that become infected differentiate into B220^{low} plasmablasts during the MMTV(SW)-encoded SAg-mediated B cell response. This early B cell differentiation was accompanied by B220 and CD62L down-regulation and by the up-regulation of CD43 and syndecan-1. Therefore, B220^{low} plasmablasts are IgD$^-$ CD62L$^-$ CD43$^+$ syndecan-1$^+$, whereas most B220^{high} B cells are CD62L$^+$ IgD$^+$ CD43$^-$ syndecan-1$^-$. Interestingly, the B220 vs MHC II profile of PO-LN CD62L$^-$ cells and CD43$^+$ cells at day 6 after MMTV(SW) injection (Fig. 2*B*) revealed that ~8–10% of CD62L$^-$ CD43$^+$ B cells had not down-regulated B220 by day 6, and, therefore, were found within the B220^{high} B cell subset.

PCR analysis, using primers specific for endogenous as well as exogenous MMTV sequences of the B220^{low} and B220^{high} B cell subpopulations isolated on days 5–7 by FACS, showed that viral DNA could be detected on the B220^{low} but not on the B220^{high} B cells; two to three copies of MMTV(SW) were found per B220^{low} B cell. In fact, as illustrated in Fig. 3, in which the presence of viral DNA is shown for different cell subsets, when total PO-LN cells from control mice or total PO-LN B220^{high} plasmablasts isolated at day 6 after MMTV infection were analyzed, no viral DNA was detected, whereas a strong signal was obtained for day 6 PO-LN B220^{low} plasmablasts. Interestingly, MMTV DNA could be detected in sorted blast B220^{high} B cells but not in small B220^{high} B cells. This is most likely due to the fact that a small proportion of blast CD62L$^-$ CD43$^+$ B cells containing MMTV-infected cells, which had not yet down-regulated B220, was still present at day 6 within the B220^{high} B cell subset (see Fig. 2*B*). Analysis of the kinetics of the B220^{low} CD62L$^-$ CD43$^+$ B cell subset revealed that CD62L$^-$ CD43$^+$ blast cells were no longer present within B220^{high} B cells after day 7 (data not shown), indicating that CD62L$^-$ CD43$^+$ B cell blasts had down-regulated B220 or had migrated from the lymph node at this time point. Therefore, B220^{low} plasmablasts represent the vast majority of the infected B cell population amplified as a result of the SAg-specific Th cell-mediated B cell proliferation response.

Systemic immune response to MMTV(SW)

Analysis of the percentage of cycling cells, Vβ6$^+$ cells, and CD69$^+$ cells within the B cell and T cell compartments indicated that these parameters did not undergo significant variations in the inguinal and mesenteric lymph nodes, Peyer's patches, and spleen after MMTV(SW) injection (data not shown), and, therefore, that an immune response against the virus was not mounted in these organs. However, there was a small but significant increase in the percentage of B220^{low} plasmablasts after MMTV(SW) injection in the mesenteric lymph nodes (MS-LN) (Fig. 4) and spleen, but not in the inguinal lymph nodes or in the Peyer's patches (data not

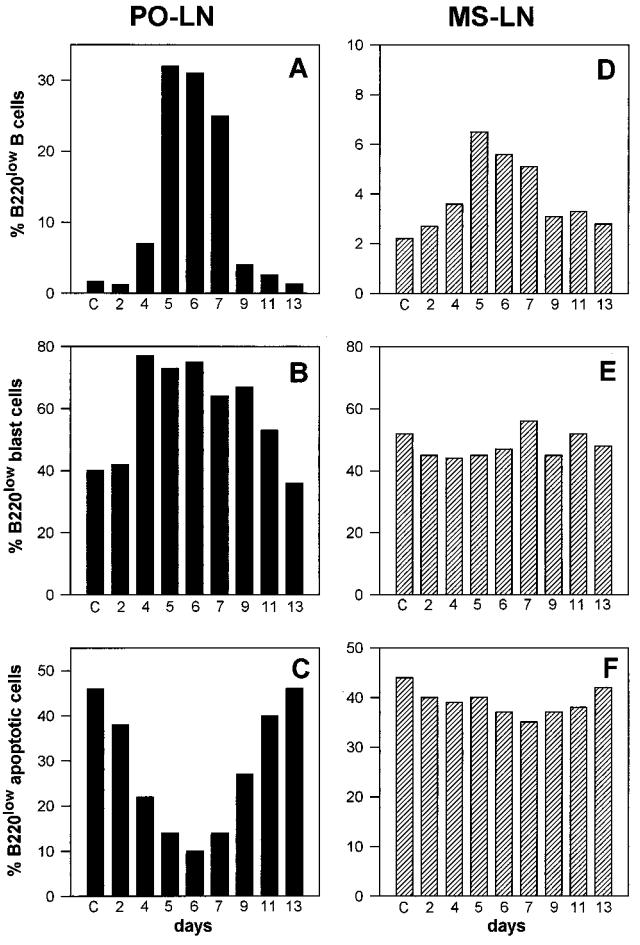

FIGURE 4. Comparative analysis of $B220^{low}$ plasmablasts in the draining PO-LN and in the nondraining MS-LN. Percentages of $B220^{low}$ B cells among B cells (*A* and *D*), of blast cells within $B220^{low}$ B cells (*B* and *E*), and of apoptotic cells within $B220^{low}$ B cells (*C* and *F*) at the indicated times after MMTV(SW) injection are shown.

shown). Analysis of the percentage of apoptotic cells within the $B220^{low}$ population in the PO-LN during the B cell response to MMTV(SW) (Fig. 4, *B* and *C*) revealed an inverted correlation between cycling and apoptotic cells (i.e., the peak of cycling cells coincided with the lowest percentage of apoptotic cells). Interestingly, in the MS-LN and spleen, the $B220^{low}$ plasmablast population did not show variations in the percentage of blast and apoptotic cells, which remained at the control levels found in the PO-LN before and after the $B220^{low}$ B cell response. These data suggest that no proliferation occurs in these locations within this B cell population, and, therefore, that the increase in the number of $B220^{low}$ plasmablasts in the MS-LN and spleen might be the result of the migration of these cells from the responding PO-LN.

Microscopic study of the PO-LN after MMTV(SW) infection

Fig. 5 shows the histological study of PO-LN from control mice and from mice at days 6 and 11 after injection of MMTV(SW). Although the deep cortical areas and the medullary cords were occupied almost exclusively by small resting lymphocytes in control mice (Fig. 5*A*), the vast majority of the cells infiltrating these areas were lymphoblasts, plasmablasts, and plasma cells at 6 days after MMTV(SW) injection (Fig. 5*B*). Moreover, an important number of these cells were observed in the vascular space of the medullary sinuses at this time point (Fig. 5*D*). Fig. 5*C* shows that in these same areas at 11 days after injection, macrophages, dead cells, and a few blast cells were observed, indicating that the decline of the B and T cell response was accompanied by a certain degree of cell death and by dead cell removal by phagocytes.

Analysis by electron microscopy of sorted $B220^{low}$ B cells showed that this population was heterogeneous and contained responding B cells in different phases of differentiation (i.e., B lymphoblasts, plasmablasts, and plasma cells (data not shown)) comparable with the cells observed in situ in the deep cortical areas and the medullary cords of the PO-LN 6 days after virus injection (Fig. 5*E*). Interestingly, some of the $B220^{low}$ cells contained numerous type-A viral particles of 65–75 nm in size in their cytoplasm (Fig. 5*F*), indicating that viral replication most likely occurs in these cells after MMTV(SW) infection.

Transmission of MMTV to the mammary gland

The data presented in this report, dealing with the detection of MMTV DNA and MMTV type-A particles in $B220^{low}$ B cells, suggest that this B cell population might be involved in virus transmission to the mammary gland, and, therefore, to the offspring. To test this hypothesis, we have analyzed the transmission of MMTV to the offspring of females injected before mating with $CD62L^-$ $CD43^+$ plasmablasts, $CD62L^+$ $CD43^-$ B cells, or total T cells isolated from infected mice. MMTV(SW) SAg presentation in the injected females and infection by MMTV of their offspring were detected by analyzing the deletion of MMTV(SW) SAg-reactive $V\beta6^+$ $CD4^+$ T cells (Fig. 6). For this assay, the purification of the $B220^{low}$ and $B220^{high}$ B cell subsets has been performed by isolating $CD62L^-$ $CD43^+$ and $CD62L^+$ $CD43^-$ B cells, respectively, because, as shown in Fig. 2*B*, a small proportion of $CD62L^-$ $CD43^+$ B cells, which could potentially contain MMTV-infected cells, exists at day 6 within the $B220^{high}$ B cells (see *Materials and Methods* for details). Females injected with $CD62L^-$ $CD43^+$ plasmablasts but not with $CD62L^+$ $CD43^-$ B cells, T cells, or control total PO-LN cells (data not shown) underwent a strong deletion of $V\beta6^+$ $CD4^+$ T cells (Fig. 6*A*), suggesting that MMTV(SW) SAg-presenting plasmablasts persisted for a long period of time or infected other cells upon injection in an appropriate host. In addition, a strong deletion of $V\beta6^+$ $CD4^+$ T cells was observed in the offspring of the females injected with $CD62L^-$ $CD43^+$ plasmablasts (Fig. 6*B*), indicating that the litters were infected with MMTV. No $V\beta6^+$ $CD4^+$ T cell deletion was observed in the offspring of females injected with $CD62L^+$ $CD43^-$ B cells, T cells or control cells. These results demonstrate that MMTV replication occurs in the $CD62L^-$ $CD43^+$ B cell-injected females, and that $B220^{low}$ plasmablasts can transmit MMTV infection to the offspring.

Discussion

Successful infection by MMTV requires the establishment of a T cell-dependent B cell response from a susceptible host, determined by the expression of a SAg encoded by the virus (3, 13). The MMTV-SAg expressed by the infected B cells specifically stimulates $CD4^+$ T cells carrying a particular TCR Vβ-chain and therefore triggers strong T cell help, which drives a B cell response leading to the amplification of the infected B cell pool (4). This SAg-induced T cell-dependent B cell response involves extrafollicular as well as follicular B cell differentiation similar to conventional Ag responses (5, 14, 25). Although this B cell response has been shown to be necessary for an efficient infection, little is known about the mechanism of virus transmission to the mammary gland during the later phases of infection; therefore, the identity of the cells supporting the persistence of the virus is still controversial (reviewed in Ref. 14). In this sense, Tsubura et al. (26) reported 10

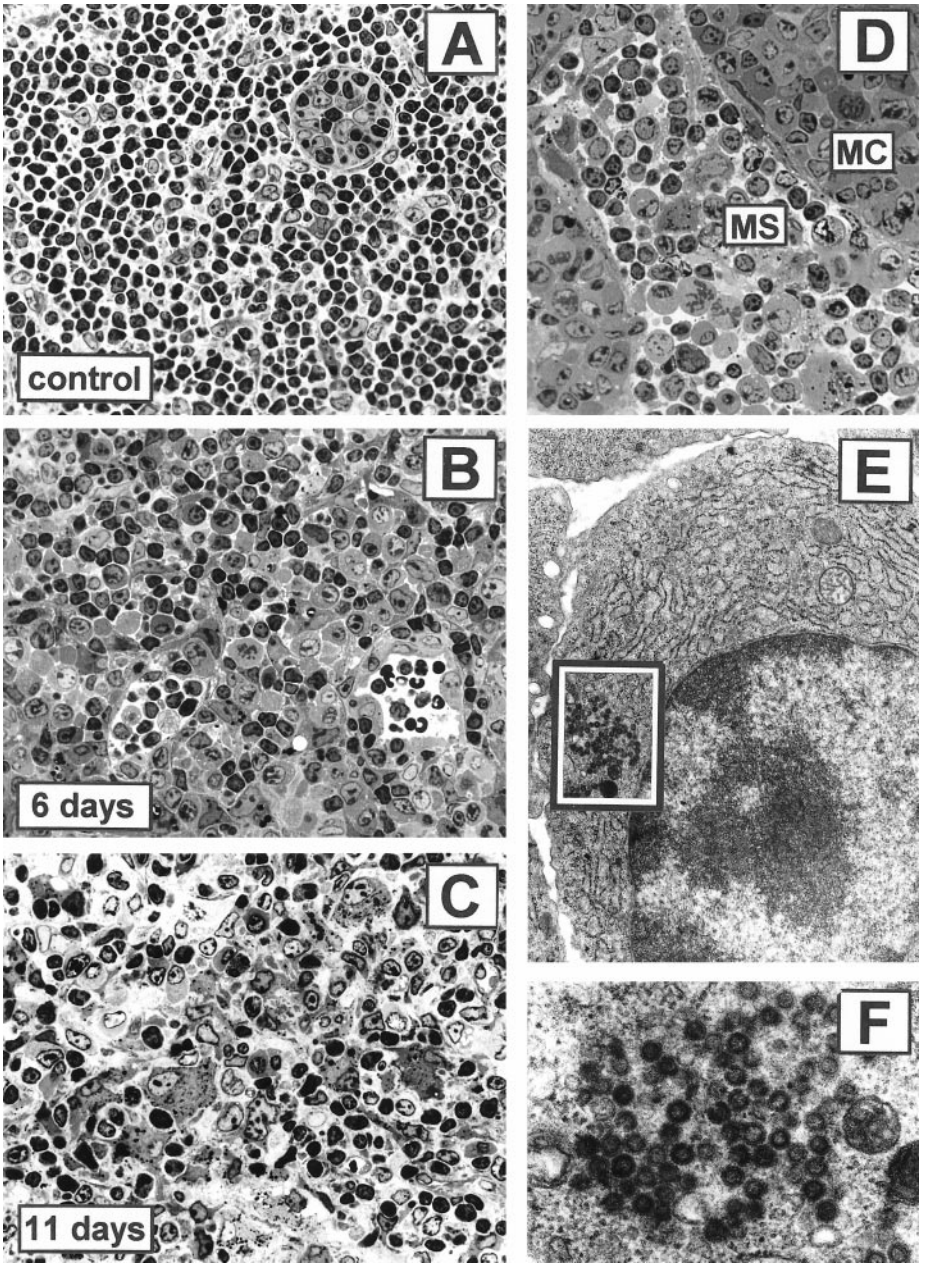

FIGURE 5. Histological study of the draining PO-LN in control mice and 6 days after injection of MMTV(SW). *A–C*, Semithin sections of the PO-LN deep cortex of control mice (*A*), mice at 6 days (*B*), or mice at 11 days (*C*) after MMTV(SW) injection (×560 magnification). *D*, Medullary cords (MC) and medullary sinus (MS) of the draining PO-LN 6 days after MMTV(SW) injection (×680 magnification). *E*, Plasmablasts located in the deep cortex of the draining PO-LN 6 days after MMTV(SW) injection. The box shows an accumulation of viral particles (×16,000 magnification). *F*, Higher magnification of the box shown in *E*, showing type-A retroviral particles 65–75 nm in size (×60,000 magnification).

years ago that transfer of T cells but not B cells from B-MMTV-infected donors resulted in mammary tumor formation in athymic nude mice. Later it was shown that transfer of both B and T cells from 6-mo-old-infected mice can induce virus transmission to the next generation (16). Recently, it has been found that both B and T cells can release infectious MMTV particles in vitro (27). Finally, Upragarin et al. (28) have proposed that the transfer of MMTV (II-TES14) from originally infected B cells to non-SAg-specific Vβ8 T cells may contribute to stable MMTV infection. In this context, to get new insights on the virus transmission, we have extensively analyzed the B cell response and the phenotype of infected cells after injection of MMTV(SW).

The immune response induced by MMTV(SW) was characterized by the activation and proliferation of B cells and MMTV-SAg reactive Vβ6$^+$ CD4$^+$ Th cells, as reported previously (4). As indicated by the analysis of the total cell number in the draining PO-LN as well as the percentage of cycling cells, activated cells, and Vβ6$^+$ CD4$^+$ T cells, the response peaked at days 6 and 7 after MMTV injection and then declined to control levels after 2 wk (data not shown). T cell help mediated by the SAg-specific Vβ6$^+$ CD4$^+$ cells drives B cell activation, proliferation, and differentiation into Ab-forming cells, which lead to the expansion of the initial number of MMTV-infected B cells (3). The pattern of the B cell response induced by MMTV correlated with the kinetics of Ab-forming cells described in the extrafollicular foci of secondary lymphoid organs (8, 9, 29).

Our results show that the immune response to MMTV involves the differentiation of plasmablasts with a high proliferation rate, characterized phenotypically by high MHC class II levels but low expression of the B cell marker B220. Down-regulation of B220 has been described previously on 4-hydroxy-3-nitrophenyl nuclear protein (NP)-specific APCs (8, 9) and after in vitro activation of B cells (30). These B220^{low} plasmablasts were first detected by day 4 postinjection, peaked by days 6 and 7 when they represented $\leq$40% of PO-LN B cells, and became barely detectable by day 9. Interestingly, PCR analysis using MMTV-specific primers has shown that viral DNA can be detected in B220^{low} B cells but not

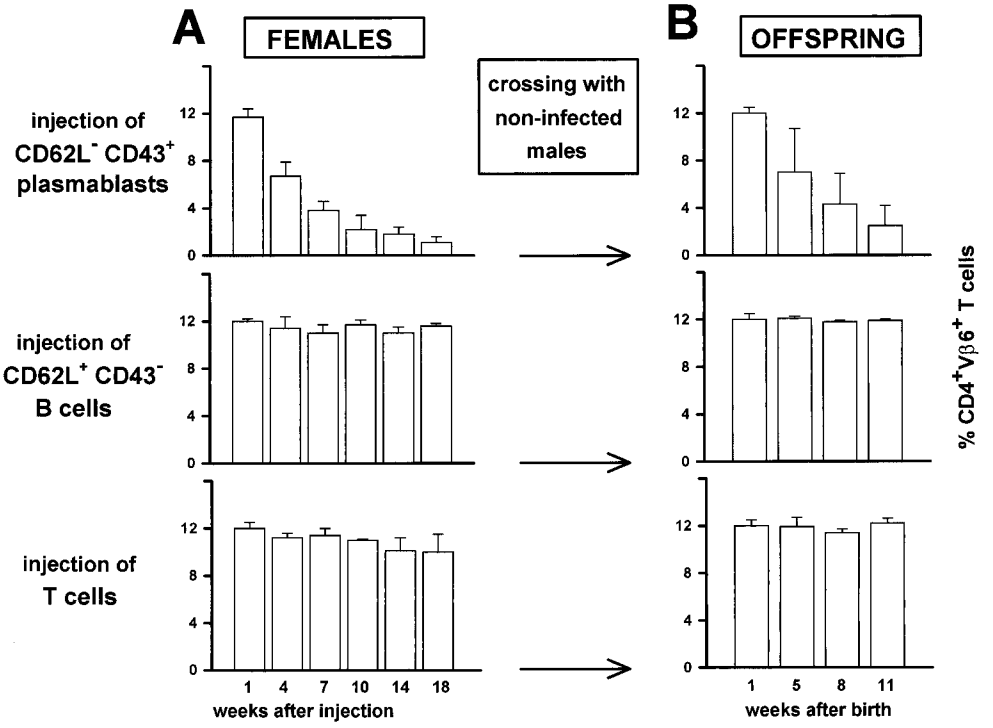

FIGURE 6. Transmission of MMTV by B220^{low} plasmablasts. *A*, CD62L$^-$ CD43$^+$ plasmablasts, CD62L$^+$ CD43$^-$ B cells, or T cells isolated from BALB/c mice 6 days after MMTV injection were transferred i.v. into BALB/c females. Deletion of Vβ6$^+$ CD4$^+$ T cells was monitored at the indicated times. Data represent the mean ± SD of the values obtained from three females for each experimental condition. *B*, At 3 months after the transfer of the indicated cell population, the females were crossed with noninfected BALB/c males. Deletion of Vβ6$^+$ CD4$^+$ T cells was analyzed in the offspring. Data represent the mean ± SD of the values obtained from the litters of each group of three females used in each experiment.

in B220^{high}-resting B cells, indicating that the B220^{low} plasmablasts represent the bulk of MMTV-infected cells during their proliferative phase.

Cell surface marker analysis of B220^{low} plasmablasts has evidenced that these cells display high levels of the adhesion molecules LFA-1 and CD44 and low levels of CD62L (i.e., an activated phenotype) (31, 32). By day 6 after MMTV injection, B220^{low} B cells expressed the B cell differentiation markers CD43 and syndecan and were IgD$^-$. These data indicate that by day 6, B220^{low} B cells represent extrafollicular plasmablasts originated by SAg-mediated differentiation of MMTV-infected B220^{high} B cells, which have switched to downstream Ig classes. Interestingly, their phenotypic profile allowed the detection and isolation of MMTV-infected cells and corresponded to that described previously for NP-specific Ab-forming cells of the splenic foci (8, 9) involved in the production of low-affinity Abs during the primary response to NP.

Electron microscopy studies of B220^{low} FACS-sorted cells have shown that the B220^{low} population is morphologically heterogeneous and includes blast and dividing cells, plasmablasts, and plasma cells. Analysis of the draining PO-LN at day 6 after MMTV injection revealed that most B220^{low} plasmablasts were localized in the deep cortical areas and in the medullary cords and sinuses. Due to the lymph flow pattern in the mouse PO-LN (33), B220^{low} plasmablasts located within the medullary sinus vascular space will most likely exit the lymph node via the efferent lymphatic and, therefore, could migrate to other peripheral lymphoid organs. Interestingly, groups of viral particles corresponding to the MMTV type-A particles described in mammary tumor epithelial cells (34) were found in the cytoplasm of FACS-sorted B220^{low} plasmablasts as well as in cells with similar morphological characteristics observed in sections of the draining PO-LN at day 6. This result suggests that viral replication can take place in these cells during the early phase of viral infection and contrasts with previous reports supporting the assertion that viral replication occurs only in later stages, when the mammary gland epithelial cells are infected. Importantly, although intracytoplasmic A particles are considered to be precursors of the core of the mature MMTV particles, it has been shown that, despite being devoid of the characteristic spikes of MMTV, they are capable of inducing mammary tumors in an appropriate host (35).

The detection of MMTV DNA and MMTV viral particles in B220^{low} plasmablasts reported here suggests that this cell population may be responsible for the transmission of MMTV. In this sense, the increase in B220^{low} plasmablasts observed between days 6 and 8 after MMTV injection in the spleen and MS-LN, in which no detectable immune response to MMTV occurred, suggests that the B220^{low} plasmablasts found in these lymphoid organs originate in the draining PO-LN, and, therefore, constitute a cell population with migratory capacity. This hypothesis is in agreement with our morphological studies, demonstrating the presence of cells morphologically similar to B220^{low} plasmablasts in the medullary sinuses of the draining PO-LN. Interestingly, CD43 expression by B220^{low} plasmablasts could be related to their recirculation potential, because this molecule has been demonstrated to participate in lymphocyte homing (36).

The kinetics of Vβ6$^+$ CD4$^+$ T cell deletion occurring in females injected with CD62L$^-$ CD43$^+$ plasmablasts indicate that this cell population persisted for a long period of time after transfer and retained its SAg-presenting cell capacity or alternatively was capable of transferring infection to other lymphocyte subsets. In this sense, it has been recently reported that both B and T cells can shed infectious MMTV particles into the supernatant after in vitro culture (27). Interestingly, challenging the classical immunological dogma that holds that plasma cells are short-lived cells, two recent

reports examining the issue of the longevity of plasma cells have demonstrated that a substantial fraction of these cells are long-lived, and can survive for periods of >1 yr (10, 11).

Finally, the transfer of $CD62L^-$ $CD43^+$ plasmablasts, but not of $CD62L^+$ $CD43^-$ B cells or T cells, into noninfected females caused a strong deletion of $V\beta6^+$ $CD4^+$ T cells in the offspring, demonstrating that MMTV replication occurred in the females after injection of $CD62L^-$ $CD43^+$ plasmablasts and, more importantly, that MMTV was transmitted to the offspring.

In conclusion, our results strongly support the hypothesis that the $B220^{low}$ plasmablasts generated during the extrafollicular B cell response to MMTV(SW) may play an important role in the transmission of the virus to the mammary gland and the offspring during infection by MMTV.

Acknowledgments

We thank A. Rolink for the anti-CD40 hybridoma FGK45 (Basel Institute for Immunology, Basel, Switzerland) and P. Zaech and C. Knabenhans for their assistance with cell sorting.

References

1. Acha-Orbea, H., and H. R. MacDonald. 1995. Superantigens of mouse mammary tumor virus. *Annu. Rev. Immunol. 13:459.*
2. Karapetian, O., A. N. Shakhov, J. Kraehenbuhl, and H. Acha-Orbea. 1994. Retroviral infection of neonatal Peyer's patch lymphocytes: the mouse mammary tumor virus model. *J. Exp. Med. 180:1511.*
3. Held, W., G. A. Waanders, A. N. Shakhov, L. Scarpellino, H. Acha-Orbea, and H. R. MacDonald. 1993. Superantigen-induced immune stimulation amplifies mouse mammary tumor virus infection and allows virus transmission. *Cell 74: 529.*
4. Held, W., A. N. Shakhov, S. Izui, G. A. Waanders, L. Scarpellino, H. R. MacDonald, and H. Acha-Orbea. 1993. Superantigen-reactive $CD4^+$ T cells are required to stimulate B cells after infection with mouse mammary tumor virus. *J. Exp. Med. 177:359.*
5. Luther, S. A., A. Gulbranson-Judge, H. Acha-Orbea, and I. C. M. MacLennan. 1997. Viral superantigen drives extrafollicular and follicular B cell differentiation leading to virus-specific antibody production. *J. Exp. Med. 185:551.*
6. Liu, Y. J., G. Grouard, O. De Bouteiller, and J. Banchereau. 1996. Follicular dendritic cells and germinal centers. *Int. Rev. Cytol. 166:139.*
7. Kelsoe, G., and B. Zheng. 1993. Sites of B-cell activation in vivo. *Curr. Opin. Immunol. 5:418.*
8. Lalor, P. A., G. J. V. Nossal, R. D. Sanderson, and M. G. McHeyzer-Williams. 1992. Functional and molecular characterization of single, (4-hydroxy-3-nitrophenyl) acetyl (NP)-specific, $IgG1^+$ B cells from antibody-secreting and memory B cell pathways in the C57BL/6 immune response to NP. *Eur. J. Immunol. 22: 3001.*
9. Smith, K. G. C., T. D. Hewitson, G. J. V. Nossal, and D. M. Tarlinton. 1996. The phenotype and fate of the antibody-forming cells of the splenic foci. *Eur. J. Immunol. 26:444.*
10. Manz, R. A., A. Thiel, and A. Radbruch. 1997. Lifetime of plasma cells in the bone marrow. *Nature 388:133.*
11. Slifka, M. K., R. Antia, J. K. Whitmire, and R. Ahmed. 1998. Humoral immunity due to long-lived plasma cells. *Immunity 8:363.*
12. Held, W., G. A. Waanders, H. Acha-Orbea, and H. R. MacDonald. 1994. Reverse transcriptase-dependent and -independent phases of infection with mouse mammary tumor virus: implications for superantigen function. *J. Exp. Med. 180:2347.*
13. Golovkina, T. V., J. P. Chervonsky, J. P. Dudley, and S. R. Ross. 1992. Transgenic mouse mammary tumor virus superantigen expression prevents viral infection. *Cell 69:637.*
14. Luther, S. A., and H. Acha-Orbea. 1997. Mouse mammary tumor virus: immunological interplays between virus and host. *Adv. Immunol. 65:139.*
15. Günzburg, W. H., and B. Salmons. 1992. Factors controlling the expression of mouse mammary tumour virus. *Biochem. J. 283:625.*
16. Waanders, G. A., A. N. Shakhov, W. Held, O. Karapetian, H. Acha-Orbea, and H. R. MacDonald. 1993. Peripheral T cell activation and deletion induced by transfer of lymphocyte subsets expressing endogenous or exogenous mouse mammary tumor virus. *J. Exp. Med. 177:1359.*
17. Sarmiento, M., D. P. Dialynas, D. W. Lancki, K. A. Wall, M. I. Lorber, M. R. Loken, and F. W. Fitch. 1982. Cloned T lymphocytes and monoclonal antibodies as probes for cell surface molecules active in T cell-mediated cytolysis. *Immunol. Rev. 68:135.*
18. Yokoyama, W. M., F. Koning, P. J. Kehn, G. M. Pereira, G. Stingl, J. E. Coligan, and E. M. Shevach. 1988. Characterization of a cell surface-expressed disulfide-linked dimer involved in murine T cell activation. *J. Immunol. 141:369.*
19. Gallatin, W. M., I. L. Weissman, and E. C. Butcher. 1983. A cell-surface molecule involved in organ-specific homing of lymphocytes. *Nature 304:30.*
20. Lesley, J., and I. S. Trowbridge. 1982. Genetic characterization of a polymorphic murine cell-surface glycoprotein. *Immunogenetics 15:313.*
21. Rolink, A., F. Melchers, and J. Anderson. 1996. The SCID but not the RAG-2 gene product is required for $S\mu$-$S\epsilon$ heavy chain class switching. *Immunity 5:319.*
22. Payne, B. T. H., B. Cannon, R. Schneider, M. W. Schilham, H. Acha-Orbea, H. R. MacDonald, and H. Hengartner. 1988. Two monoclonal rat antibodies with specificity for the β-chain variable region $V\beta6$ of the murine T cell receptor. *Proc. Natl. Acad. Sci. USA 85:7695.*
23. Nicoletti, I., N. G. Migliorati, M. C. Pagliacci, F. Grignani, and C. Riccardi. 1991. A rapid and simple method for measuring thymocyte apoptosis by propidium iodide staining and flow cytometry. *J. Immunol. Methods 139:271.*
24. Ardavín, C., F. Luthi, M. Andersson, L. Scarpellino, P. Martín, H. Diggelmann, and H. Acha-Orbea. 1997. Retrovirus-induced target cell activation in the early phases of infection: the mouse mammary tumor virus model. *J. Virol. 71:7295.*
25. MacLennan, I. C. M., A. Gulbranson-Judge, K. M. Toellner, M. Casamayor-Palleja, E. Chan, D. M. Sze, S. A. Luther, and H. Acha-Orbea. 1997. The changing preference of T and B cells for partners as T-dependent antibody responses develop. *Immunol. Rev. 156:53.*
26. Tsubura, A., M. Inaba, S. Imai, A. Murakami, N. Oyaizu, R. Yasumizu, Y. Ohnishi, H. Tanaka, S. Morii, and S. Ikehara. 1998. Intervention of T-cells in transportation of mouse mammary tumor virus (milk factor) to mammary gland cells in vivo. *Cancer Res. 48:6555.*
27. Dzuris, J. L., T. V. Golovkina, and S. R. Ross. 1997. Both T and B cells shed infectious mouse mammary tumor virus. *J. Virol. 71:6044.*
28. Upragarin, N., H. Nishimura, W. Wajjwalku, Y. Ando, S. Nagafuchi, T. Watanabe, and Y. Yoshikai. 1997. T cells bearing $V\beta8$ are preferentially infected with exogenous mouse mammary tumor virus. *J. Immunol. 159:2189.*
29. Jacob, J., R. Kassir, and G. Kelsoe. 1991. In situ studies of the primary immune response to (4-hydroxy-3-nitrophenyl) acetyl: the architecture and dynamics of responding cell populations. *J. Exp. Med. 173:1165.*
30. Dustin, L. B., E. D. Bullock, Y. Hamada, T. Azuma, and D. Y. Loh. 1995. Antigen-driven differentiation of naive Ig-transgenic B cells in vitro. *J. Immunol. 154:4936.*
31. Dustin, M. L., and T. A. Springer. 1991. Role of lymphocyte adhesion receptors in transient interactions and cell locomotion. *Annu. Rev. Immunol. 9:27.*
32. Tedder, T. F., A. C. Penta, H. B. Levine, and A. S. Freedman. 1990. Expression of the human leukocyte adhesion/homing molecule, LAM-1: identity with the TQ1 and leu-8 differentiation antigens. *J. Immunol. 144:532.*
33. Kowala, M. C., and G. I. Schoefl. 1986. The popliteal lymph node of the mouse: internal architecture, vascular distribution, and lymphatic supply. *J. Anat. 148:25.*
34. Hageman, P. C., J. Calafat, and J. Hilgers. 1981. The biology of the mouse mammary tumor virus. In *Mammary tumors in the mouse.* J. Hilgers and M. Sluyser, eds. Elsevier Biomedical Press, Amsterdam, p. 391.
35. Nusse, R., L. van der Ploeg, L. van Duijn, R. Michalides, and J. Hilgers. 1979. Impaired maturation of mouse mammary tumor virus precursor polypeptides in lymphoid leukemia cells, producing intracytoplasmic A particles and no extracellular B-type virions. *J. Virol. 32:251.*
36. McEvoy, L. M., H. L. Sun, J. G. Frelinger, and E. C. Butcher. 1997. Anti-CD43 inhibition of T cell homing. *J. Exp. Med. 185:1493.*